

Carbon allotropes with triple bond predicted by first-principle calculation: Triple bond modified diamond and *T*-carbon

Jun Young Jo and Bog G. Kim*

Department of Physics, Pusan National University, Pusan 609-735, South Korea

(Received 19 May 2012; revised manuscript received 28 July 2012; published 28 August 2012)

We have designed new structures of carbon allotropes combining a mixture of sp (triple bond) and sp^3 (single bond) hybridization through first-principle calculation. These two structures named yne-carbon (Y-carbon) and tetrayne-carbon (TY-carbon), respectively, not only maintained the cubic structure and space group ($Fd\bar{3}m$) of diamond but were also energetically more stable than recently proposed carbon allotrope, T-carbon. A phonon calculation revealed these structures to be stable, and the nature of the triple bond was illustrated by the unique phonon spectrum with an eigen-frequency of 2200 cm^{-1} . The band gap of Y-carbon was found to be larger than that of diamond, whereas the band gap of TY-carbon was smaller than that of T-carbon, which is closely related to the properties of a carbon tetrahedron. The existence of triple bonding of carbon is associated with a dimerization phenomenon due to Peierls instability.

DOI: [10.1103/PhysRevB.86.075151](https://doi.org/10.1103/PhysRevB.86.075151)

PACS number(s): 64.60.My, 71.15.Mb, 71.20.Mq, 81.05.Zx

I. INTRODUCTION

Carbon is one of the most familiar and important elements in the periodic table. Recently, there has been renewed interest in carbon allotropes,^{1–6} which is expected to create technological breakthroughs that will have significant impacts on future life and industry. The evaluation of carbon often came with the discovery of carbon allotropes as the synthesis technology of modern science developed. In 1985, Kroto *et al.* discovered buckminsterfullerene (C_{60}).¹ This was soon followed by structural identification carbon nanotubes in 1991 by Iijima.² In 2004, Novoselov *et al.* realized isolation of carbon allotrope with a two-dimensional structure, called graphene.^{3,4} Carbon nanotubes and graphene with their unique physical properties and highly expected engineering possibilities have attracted focused attention from academia and industry.^{5,6} Interestingly, the discoveries of these carbon allotropes can be predicted through theoretical studies. In particular, design through first-principle calculations is an important method of finding carbon allotropes that allows us to predict the existence and the properties of carbon allotropes.^{7–11} Theoretically predicted carbon allotropes, such as graphene, onions, diamondoids, peapods, and scrolls have actually been synthesized. Based on this experience, considerable research effort has been made to assess potential carbon allotropes, such as band-gap engineering and strain engineering.^{12,13}

The unique but diverse physical/chemical properties of carbon elements are associated with the orbital properties of carbon atoms: the four electrons in a carbon atom can have sp , sp^2 , and sp^3 hybridization. According to the nature of hybridization, a carbon atom can have a one-dimensional (1D) (sp hybridization), two-dimensional (2D) (sp^2 hybridization), and three-dimensional (3D) (sp^3 hybridization) structure. This unique chemical bonding to structural relationship is strongly related to the diversity of properties through the range of combinations of hybridizations in actual allotropes.^{14–16} Recently, a carbon allotrope with the space group of diamond ($Fd\bar{3}m$), called T-carbon, was suggested using first-principle calculations.¹⁷ This allotrope was derived by substituting each atom in diamond with a carbon tetrahedron. The detailed

calculations showed that T-carbon is a stable allotrope of carbon with a lower density ($\sim 1.50\text{ g/cm}^3$) and has semi-conducting properties with a direct band gap of 3.0 eV.

In this study, first-principle calculations were used to develop 3D carbon allotropes by combining sp (triple bond) and sp^3 (single bond) hybridization. Two 3D carbon allotropes were obtained by inserting yne-bonding (triple bonding) into diamond and T-carbon through a symmetry consideration of the diamond and T-carbon structures. These carbon allotropes were called yne-carbon (Y-carbon) and tetrayne-carbon (TY-carbon). The structural stability and unique phonon spectrum of Y-carbon and TY-carbon are revealed by the detailed calculations. The electronic structure of Y-carbon and TY-carbon can be understood by symmetry considerations and the chemical bonding nature. These two novel carbon allotropes with a large cavity can be scientifically interesting materials and have broader technological impact. By filling noble gases such as Xe into their cavities, Y-carbon and TY-carbon will be expected to significantly increase their stiffness.¹⁸ In addition, they have the possibility to become good hydrogen gas storage because of the presence of the carbon triple bonds and the cavities.^{19,20}

II. COMPUTATIONAL DETAILS

First-principle calculations were performed using the generalized gradient approximation (GGA)²¹ to density functional theory and the projector-augmented-wave method as implemented in VASP.^{22,23} The $2s^2 2p^2$ electrons in carbon atom were regarded as valence electrons. The electronic wave functions were expanded with plane waves up to a kinetic-energy cutoff of 400 eV except for structural optimization, where a kinetic-energy cutoff of 520 eV was applied to reduce the effect of Pulay stress. Momentum space integration was performed using $8 \times 8 \times 8$ Monkhorst-Pack k -point mesh.²⁴ With the cubic diamond symmetry imposed, the lattice constants and internal coordinates were fully optimized until the residual Hellmann-Feynman forces were $< 10^{-3}\text{ eV/\AA}$. Calculations of the total energy as a function of the fixed volume were used to obtain the equation of states, and the internal atomic coordinate

was fully optimized at each given volume. A frozen phonon calculation was applied to a $2 \times 2 \times 2$ supercell using the PHONOPY program to obtain the phonon dispersion curve and phonon partial density of state.²⁵

III. RESULTS AND DISCUSSION

Diamond has a unique structure, which is symmetrical in 3D forming a regular tetrahedron centered on carbon atoms with sp^3 hybridization among carbon atoms. The space group of diamond is $Fd\bar{3}m$ (space group No. 227) and the possible Wyckoff positions of this space group are $8a$, $8b$, $16c$, $32e$, $48f$, $96g$, $96h$, and $192i$, into which an atom may enter. In the diamond form of carbon, the carbon atoms are located in the $8a$ (0,0,0) sites.²⁶ For T-carbon, the space group is the same as diamond but the carbon atoms are located in $32e$ (x,x,x) sites, forming a carbon tetrahedron. A simplistic variation of the diamond structure is the formation of a triple bond between carbon atoms but maintaining the space group symmetry. By inserting carbon triple bonds, two structures were optimized from diamond and T-carbon, respectively. Since the triple bond of carbon is called the yne-bond, our two optimized structures can be called yne-carbon (Y-carbon, derived from diamond) and tetrayne-carbon (TY-carbon, derived from T-carbon).

Figure 1 shows the structure of two carbon allotropes, Y-carbon and TY-carbon. Figures 1(a) and 1(b) describe the optimized structure of Y-carbon in detail. Although the carbon atoms in $8a$ (0,0,0) site form sp^3 hybridization, the carbon atoms located at the vertex $32e$ (0.0888,0.0888,0.0888) site form sp hybridization. The carbon atoms located at one vertex are expected to form a triple bond with the carbon atoms located at the other vertex of the neighboring carbon tetrahedron (indicated in orange). Figures 1(c) and 1(d) show

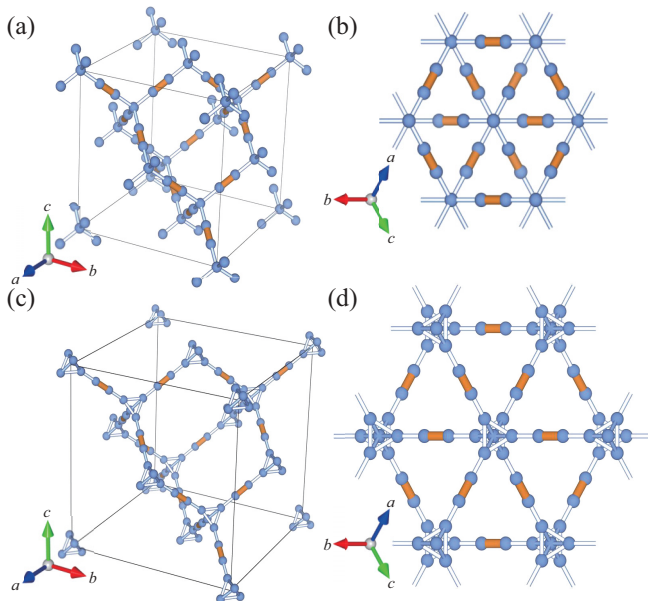


FIG. 1. (Color online) The detailed structure of (a) Y-carbon and (b) its [111] projection. The detailed structure of (c) TY-carbon and (d) its [111] projection. Triple bonds are shown as an orange cylinder and arrows indicate three basis vectors.

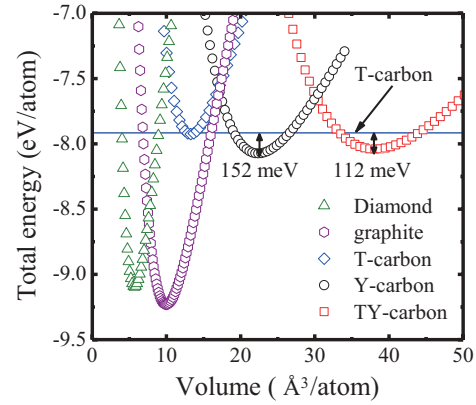


FIG. 2. (Color online) The total energy vs volume (equation of state) of diamond (green triangle), graphite (purple hexagon), T-carbon (blue square), Y-carbon (black circle), and TY-carbon (red square) calculated at the GGA level. The blue line indicates the equilibrium energy of T-carbon.

the optimized structure of TY-carbon. In this structure, carbon atoms are located in the $32e$ (0.0397,0.0397,0.0397) and $32e$ (0.0987,0.0987,0.0987) sites. The carbon atoms at the inner $32e$ (0.0397,0.0397,0.0397) site form a carbon tetrahedron with sp^3 hybridization, whereas the carbon atoms at the outer $32e$ (0.0987,0.0987,0.0987) site are linked to a carbon triple bond with an intracarbon network.

The equation of state was calculated to check the equilibrium volume. Figure 2 shows the total energy per carbon atom as a function of the volume for Y-carbon and TY-carbon at the GGA level, respectively. Both have one equilibrium point in the equation of state, suggesting their structural stability in cubic diamond symmetry. For comparison, the equilibrium energy of T-carbon was also obtained under similar conditions and plotted as a solid line. In the calculation, the equilibrium total energy per atom of T-carbon, Y-carbon, and TY-carbon was -7.922 ,¹⁷ -8.074 , and -8.034 eV/atom, respectively. In terms of the total energy, both Y-carbon and TY-carbon are more stable than T-carbon: The total energy per carbon atom of Y-carbon and TY-carbon is 152 and 112 meV/atom lower than T-carbon. On the other hand, the total energy of T-carbon, Y-carbon, and TY-carbon is higher than that of diamond and graphite, suggesting the metastable character of these carbon allotropes. Table I lists the structural parameters optimized through first-principle calculations at the GGA level.

The dynamic stability of Y-carbon and TY-carbon can be checked using phonon calculations. Figures 3(a) and 3(b) depict the phonon dispersion and phonon partial density of state of Y-carbon and TY-carbon, respectively. First of all, there was no imaginary frequency phonon in both structures, meaning the structural stability of the optimized phase against symmetry breaking. At the zone center, Y-carbon has 30 phonon modes (seven triply degenerate modes, two doubly degenerate modes, two single modes, and three acoustic modes) and TY-carbon has 48 phonon modes (11 triply degenerate modes, four doubly degenerate modes, two singly degenerate modes, and three acoustic modes). The energy eigenvalue of the phonon mode for the two structures can be explained easily by considering the bonding nature, i.e., single and triple bonds of carbon

TABLE I. The lattice constant (l), position of carbon atom (x_1, x_2), single bond length (d_s), triple bond length (d_t), equilibrium density (ρ), energy gap (E_g), and bulk modulus (BM) of cubic diamond, Y-carbon, T-carbon, and TY-carbon, respectively.

Structure	l	x_1	x_2	d_s	d_t	E_g (eV)	BM (GPa)	ρ (g/cm ³)
c-diamond	3.574	0		1.547		4.118	432	3.496
Y-carbon	9.636	0	0.0888	1.482	1.209	4.662	82.9	0.894
T-carbon	7.517	0.0706		1.501, 1.416		2.234	159	1.503
TY-carbon	13.460	0.0397	0.0987	1.510, 1.377	1.226	1.465	54.2	0.523

with different carbon-carbon lengths (intercarbon lengths are summarized in Table I). For Y-carbon, the phonon bands are characterized by a single bond (~ 1200 cm⁻¹) of carbons with an intercarbon distance of 1.482 Å and by a triple bond (~ 2300 cm⁻¹) of carbon with an intercarbon distance of 1.209 Å. Triple bonding of TY-carbon has a longer intercarbon distance of 1.226 Å and the phonon band was approximately 2200 cm⁻¹, which is a lower energy than that of the triple bonding in Y-carbon. In contrast to Y-carbon, for TY-carbon, there were two types of single bonding (see Table I), with an intercarbon length of 1.510 and 1.377 Å, respectively. The longer bonding (1.510 Å) is the bonding among carbon atoms in a carbon tetrahedron, and the shorter bonding (1.377 Å) is the bonding between the carbon atoms of a tetrahedron and the carbon atoms involved in triple bonding.

Because of the two distinct natures of carbon single bonding, the phonon band is split into two groups; shorter bonding with an energy of ~ 1200 – 1800 cm⁻¹ and longer bonding with an energy of ~ 800 cm⁻¹. The bonding length of shorter bonding is similar to that of the double bonding observed in many carbon compounds.²⁷ The above statement can be also confirmed from the phonon partial density of state (PPDOS) of Y-carbon and TY-carbon. For Y-carbon, the carbon atoms located in the $8a$ (0,0,0) site [shown by a green line in Fig. 3(a)] contribute mainly to the phonon at ~ 1200 cm⁻¹ and the carbon atoms at the $32e$ (0.0888,0.0888,0.0888) site [shown by an orange dashed line in Fig. 3(a)] contribute mainly to the phonon with an energy of ~ 2200 cm⁻¹. Again for TY-carbon, two distinct carbon atoms from two different

$32e$ Wyckoff sites contribute to two distinct phonon energy ranges, as shown in Fig 3(b) (green line and orange dashed lines). Below 590 cm⁻¹, one can also find the external mode of carbon atoms, which is a combination of the single and triple bonding of carbon atoms in Y-carbon and TY-carbon. In addition, with the exception of the phonon bands from triple bonding, the phonon spectrum of TY-carbon is quite similar to that of T-carbon and that of Y-carbon is quite similar to that of diamond.^{17,28}

X-ray diffraction (XRD) is an excellent technique for analyzing newly synthesized materials. The XRD patterns of Y-carbon and TY-carbon were simulated, and the data is summarized in Fig. 4. In this figure, the diamond, T-carbon, Y-carbon, and TY-carbon were optimized with the GGA level of first-principle calculations. Each optimized structure was then used to obtain a simulated XRD pattern using the FULLPROF package;²⁹ the x-ray wavelength was assumed to be 1.5406 Å (Cu $K\alpha_1$). In diamond, four peaks with Miller indices of (111), (220), (311), and (222) were found up to $100^\circ 2\theta$, and the strongest peak for diamond was (111). Table I lists the lattice constant of each carbon allotrope. Because the space group ($Fd\bar{3}m$) of Y-carbon and TY-carbon is the same as that of T-carbon and diamond, the shape and characteristics of the XRD pattern were similar. The main difference in the XRD pattern among carbon allotropes was the location of the XRD peak, which is a function of the inverse of the lattice constant (Bragg equation; $\lambda = 2d \sin \theta$). The position (2θ) of the strongest XRD peak for Y-carbon and TY-carbon was 15.917° and 11.377° , respectively. The relative intensity of each XRD peak is related to the structure factor of XRD and can be simulated easily with the information provided in Table I.

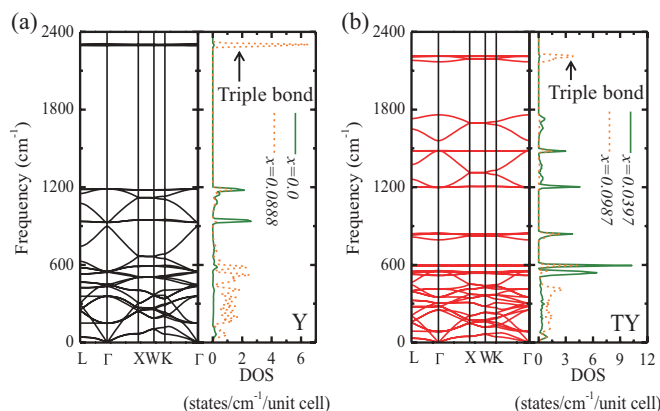


FIG. 3. (Color online) The phonon dispersion curve and partial phonon density of states of (a) Y-carbon and (b) TY-carbon, respectively. Note that the spectrum due to triple bonding occurs at around 2200 cm⁻¹.

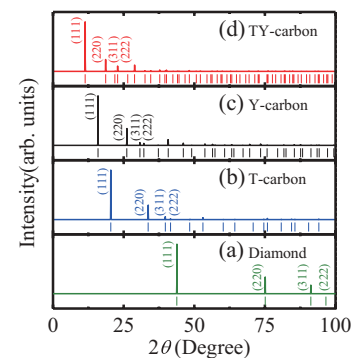


FIG. 4. (Color online) The simulated XRD ($\lambda = 1.5406$ Å) patterns of (a) diamond, (b) T-carbon, (c) Y-carbon, and (d) TY-carbon, respectively.

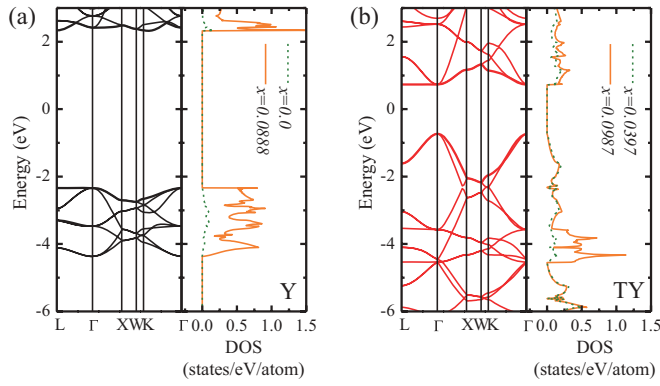


FIG. 5. (Color online) Electronic band structure along the high symmetry point in the Brillouin zone and atom projected density of states of (a) Y-carbon and (b) TY-carbon.

Having all the information on the structure and stability, the electronic structures of Y-carbon and TY-carbon can be discussed. Their band structure and atom projected density of states (PDOS) were calculated at the GGA level, as shown in Fig. 5. First of all, the overall band shape of Y-carbon was similar to that of diamond, and that of TY-carbon was similar to that of T-carbon (see Supplemental Material³³). In addition, Y-carbon has an indirect band gap, whereas TY-carbon has a direct band gap. This is because of the structural similarity, i.e., Y-carbon is believed to be a triple-bonding combination with diamond, and TY-carbon is a triple-bonding combination with T-carbon. One of the main differences is the band gap (summarized in Table I). Although the band gap of Y-carbon (4.662 eV) appeared to be larger than that of diamond (4.118 eV), the band gap of TY-carbon (1.465 eV) was smaller than that of T-carbon (2.234 eV). The optical absorption coefficient of Y-carbon and TY-carbon was calculated using electronic structure information, too (see Supplemental Material³³).

The band gap is associated with the orbital nature of carbon atoms, particularly $2s$ and $2p$ orbitals. For Y-carbon, there appears to be two distinct orbitals of carbon atoms, depending on the Wyckoff positions of $8a$ (0,0,0) and $32e$ (0.0888,0.0888,0.0888). Similar to the carbon orbital in diamond, the orbital of the carbon atom in the Wyckoff positions of $8a$ (0,0,0) forms sp^3 -like hybridization, where $2s$, $2p_x$, $2p_y$, and $2p_z$ are equivalent. On the other hand, the carbon atoms in Wyckoff positions of $32e$ (0.0888,0.0888,0.0888) form sp -like hybridization, where $2s$, $2p_x$, $2p_y$, and $2p_z$ are not equal. The $2s$ and $2p_z$ orbitals form σ bonding, whereas $2p_x$ and $2p_y$ orbitals form π bonding. Therefore, in sp -like hybridization, the electrons in each tetrahedron are more localized and the band gap of Y-carbon (4.662 eV) is larger than that of diamond (4.118 eV).

For TY-carbon, the orbital symmetry of carbon atoms is completely different from that of the carbon atoms in Y-carbon. Two distinct carbon atoms are in the same symmetric Wyckoff position with different coordinates, $32e$ (0.0397,0.0397,0.0397) and $32e$ (0.0987,0.0987,0.0987). The orbital of the carbon atoms in $x = 0.0987$ has similar character to triple bonding of sp -like hybridization, and that of the carbon atoms in $x = 0.0397$ has similar character to

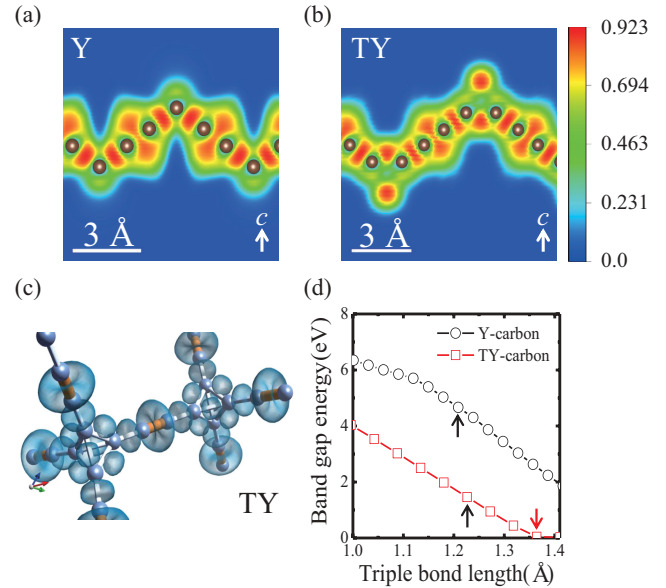


FIG. 6. (Color online) The ELF of (a) Y-carbon and (b) TY-carbon along the carbon chain. (c) ELF of TY-carbon viewed in 3D (contour level is set to 0.75). (d) The calculated band gap of Y-carbon and TY-carbon as a function of triple bond length, showing Peierls instability in TY-carbon.

single-bonding sp^3 -like hybridization. On the other hand, the carbon atoms of TY-carbon in $x = 0.0397$ have $32e$ symmetry, which is not equal to the $8a$ symmetry of Y-carbon. The orbitals of the carbon atoms are distributed asymmetrically along the carbon tetrahedron due to symmetry constraints. The symmetry difference can be the origin of the different trend of the band gap in Y-carbon and TY-carbon. These characteristics can be seen by the atom PDOS. For Y-carbon, valence band maximum (VBM) and conduction band minimum (CBM) are composed mainly of electrons in the $32e$ site and the contribution from the electron in the $8a$ site is quite small. On the other hand, for TY-carbon, two electrons from different $32e$ sites contribute to the VBM and CBM.

The bonding nature of electrons can be checked by electron localization function (ELF) analysis³⁰ [Figs. 6(a), 6(b), and 6(c)]. Figures 6(a) and 6(b) show the $(\bar{1}10)$ cross sections of ELF along the carbon chain of Y-carbon and TY-carbon, respectively. For Y-carbon, the electrons are well localized along the carbon chain, and the enhanced localization between triple bonded carbons can be seen clearly. On the other hand, for TY-carbon, the electron localization along the triple bond is weakened compared to that of Y-carbon. In addition, the electrons formed by the tetrahedron are squeezed out rather than distributed inside the tetrahedron or on the line of the tetrahedron. This phenomenon can be clarified in the three-dimensional plot of the ELF of TY-carbon, as shown in Fig. 6(c). The ELF function around the tetrahedron is distributed nonuniformly along the bonding lines of the tetrahedron.

Because triple bonding between carbon atoms is an important ingredient of yne modification, the length of the triple bond (d_t) is closely related to the band gap of both Y-carbon and TY-carbon. The band gap as a function of the triple bond length can be obtained by maintaining the same lattice constant, and is depicted in Fig. 6(d). The equilibrium bond

length (d_{t0}) is denoted by the black arrow and d_{t0} of Y-carbon and TY-carbon is 1.2086 Å and 1.2263 Å, respectively. As d_t is increased from 1 to 1.4 Å, the band gap of both materials decreases monotonically. For Y-carbon, it is still in the insulating state with a finite band gap at 1.4 Å. On the other hand, for TY-carbon, the band-gap energy decreases with increasing d_t . Eventually, the band gap is closed when the d_t reaches 1.364 36 Å, and an insulator to metal transition occurs. This phenomenon in TY-carbon is related closely to Peierls instability.^{31,32} Triple bond formation with a linear carbon chain is a well-known example of Peierls instability leading to the dimerization of carbon. In other words, in TY-carbon, the metallic state can be the ground state if the bond length between the triple bonded carbons is similar to that of single bonded carbon. On the other hand, dimerization between carbon atoms can occur due to Peierls instability, which is responsible for the insulating band gap of TY-carbon. One should note that dimerization in TY-carbon occurs in a 3D manner because of its structure, which can be thought of as a 1D Peierls-like transition along a linear carbon chain in 3D networks (see Supplemental Material³³).

IV. CONCLUSIONS

In conclusion, this study designed carbon allotropes with yne modification, named Y-carbon and TY-carbon. These

structures can be made with the combination of sp^3 and sp hybridization, which maintain the same space group ($Fd\bar{3}m$) of cubic diamond and T-carbon. Both allotropes can be stable with the total energy in lower equilibrium than that of T-carbon. Their kinetic stability can also be confirmed by phonon calculation and the phonon spectrum of Y-carbon and TY-carbon can be explained easily by the combination of sp^3 and sp hybridization. The band gaps of both Y-carbon and TY-carbon can also be understood by the coexisting single and triple bonding of the carbon atoms. The band gap of TY-carbon can be modified to become a metal, which can be explained by Peierls instability associated with the dimerization of carbon atoms. Stable carbon allotropes with a larger pore volume can be scientifically interesting materials and have a broader technological impact as a very hard material¹⁸ and hydrogen storage.^{19,20}

ACKNOWLEDGMENTS

The authors wish to thank R. Baughman for the helpful discussions and encouragement during the initial state of this work. This study was supported by NSF of Korea (KRF-2012-0000964 and KRF-2012-0004688). Computational resources were provided by the KISTI Supercomputing Center (Project No. KSC-2011-C1-20).

*boggikim@pusan.ac.kr

- ¹H. W. Kroto, J. R. Heath, S. C. O'Brien, R. F. Curl, and R. E. Smalley, *Nature (London)* **318**, 162 (1985).
- ²S. Iijima, *Nature (London)* **354**, 56 (1991).
- ³K. S. Novoselov, A. K. Geim, S. V. Morozov, D. Jiang, Y. Zhang, S. V. Dubonos, I. V. Grigorieva, and A. A. Firsov, *Science* **306**, 666 (2004).
- ⁴A. K. Geim and K. S. Novoselov, *Nat. Mater.* **6**, 183 (2007).
- ⁵S. Sanvito, *Nat. Mater.* **10**, 484 (2011).
- ⁶M. Urdampilleta, S. Klyatskaya, J. P. Cleuziou, M. Ruben, and W. Wernsdorfer, *Nat. Mater.* **10**, 502 (2011).
- ⁷K. S. Novoselov, A. K. Geim, S. V. Morozov, D. Jiang, M. I. Katsnelson, I. V. Grigorieva, S. V. Dubonos, and A. A. Firsov, *Nature (London)* **438**, 197 (2005).
- ⁸H. W. Kroto, *Nature (London)* **359**, 670 (1992).
- ⁹J. E. Dahl, S. G. Liu, and R. M. K. Carlson, *Science* **299**, 96 (2003).
- ¹⁰B. W. Smith, M. Monthieux, and D. E. Luzzi, *Nature (London)* **396**, 323 (1998).
- ¹¹J. L. Li, Q. S. Peng, G. Z. Bai, and W. Jiang, *Carbon* **43**, 2830 (2005).
- ¹²S.-H. Lee, H.-J. Chung, J. Heo, H. Yang, J. Shin, U-In Chung, and S. Seo, *ACS Nano*, **5**, 2964 (2011).
- ¹³R. Mitsunashi, Y. Suzuki, Y. Yamanari, H. Mitamura, T. Kambe, N. Ikeda, H. Okamoto, A. Fujiwara, M. Yamaji, N. Kawasaki, Y. Maniwa, and Y. Kubozono, *Nature (London)* **464**, 76 (2010).
- ¹⁴R. H. Baughman, H. Eckhardt, and M. Kertesz, *J. Chem. Phys.* **87**, 6687 (1987).
- ¹⁵H. R. Karfunkel and T. Dressler, *J. Am. Chem. Soc.* **114**, 2285 (1992).

¹⁶A. Hirsch, *Nat. Mater.* **9**, 868 (2010).

- ¹⁷X.-L. Sheng, Q.-B. Yan, F. Ye, Q.-R. Zheng, and G. Su, *Phys. Rev. Lett.* **106**, 155703 (2011).
- ¹⁸L. Itzhaki, E. Altus, H. Basch, and S. Hoz, *Angew. Chem.* **44**, 7432 (2005).
- ¹⁹P. B. Sorokin, H. Lee, L. Y. Antipina, A. K. Singh, and B. I. Yakobson, *Nano Lett.* **11**, 2660 (2011).
- ²⁰C. Li, J. Li, F. Wu, S.-S. Li, J.-B. Xia, and L.-W. Wang, *J. Chem. Phys.* **119**, 2376 (2003).
- ²¹J. P. Perdew, K. Burke, and M. Ernzerhof, *Phys. Rev. Lett.* **77**, 3865 (1996); **78**, 1396(E) (1997).
- ²²G. Kresse and J. Furthmuller, *Phys. Rev. B* **54**, 11169 (1996).
- ²³G. Kresse and D. Joubert, *Phys. Rev. B* **59**, 1758 (1999).
- ²⁴H. J. Monkhorst and J. D. Pack, *Phys. Rev. B* **13**, 5188 (1976).
- ²⁵A. Togo, F. Oba, and I. Tanaka, *Phys. Rev. B* **78**, 134106 (2008).
- ²⁶*International Tables for Crystallography*, Vol. A, 5th ed. (The International Union of Crystallography, Springer, Norwell, 2005).
- ²⁷L. G. Wade, *Organic Chemistry*, 7th ed. (Pearson Prentice Hall, New Jersey, 2009).
- ²⁸G. Kresse, J. Furthmuller, and J. Hafner, *Europhys. Lett.* **32**, 729 (1995).
- ²⁹J. Rodriguez Carvajal, *Physica B* **192**, 55 (1993).
- ³⁰B. Silvi and A. Savin, *Nature (London)* **371**, 683 (1994).
- ³¹R. E. Peierls, *Quantum Theory of Solids* (Clarendon, Oxford, 1955).
- ³²R. E. Peierls, *More Surprises in Theoretical Physics* (Princeton University, Princeton, 1991).
- ³³See Supplemental Material at <http://link.aps.org/supplemental/10.1103/PhysRevB.86.075151> for the detailed calculations about electronic structure, optical absorption, and Peierls transition.